Polyhedron 222 (2022) 115917

Contents lists available at ScienceDirect

Polyhedron

journal homepage: www.elsevier.com/locate/poly

Coordination modes of hydrazone and acyl-hydrazone ligands containing a pyridine group with the $\{Re(CO)_3\}^+$ fragment

Saray Argibay [a,b], Diego Costas-Riveiro [a], Rosa Carballo [a,b], Ezequiel M. Vázquez-López [a,b,*]

[a] Universidade de Vigo, Departamento de Química Inorgánica, Facultade de Química, 36310 Vigo, Spain
[b] Metallosupramolecular Chemistry Group, Galicia Sur Health Research Institute (IIS Galicia Sur). SERGAS-UVIGO, Galicia, Spain

ARTICLE INFO

Dedicated to Prof. Ionel Haiduc, at his 85th birthday.

Keywords:
Rhenium(I) complexes
Hydrazone
Acyl-hydrazone
Zwitterion
Crystal structure

ABSTRACT

Four acyl-hydrazones derived from 5-hydroxypicolinohydrazide and 4-hydroxybenzaldehyde (**HL^{11}**), 2-fluoro-4-hydroxybenzaldehyde (**HL^{12}**), 2,4-dihydroxybenzaldehyde (**HL^{13}**) or 2-pyridinecarboxaldehyde (**HL^{14}**) and two hydrazones derived from 2-hydrazino pyridine and 4-dimethylaminobenzaldehyde (**HL^{21}**) or 4-diethylamino-2-hydroxybenzaldehyde (**HL^{22}**) were synthesized and their X-ray structures determined. Twelve rhenium(I) complexes of formula $[ReX(HL^n)(CO)_3]$ (X = Cl, Br) were obtained by treating these ligands with $[ReX(CH_3CN)_2(CO)_3]$, and the structures of some representative compounds were determined by X-ray diffraction.

The coordination geometry around rhenium(I) can be described as octahedral, with three carbon atoms in a *fac* configuration, the halogen atom and two nitrogen atoms from the hydrazone chain and the pyridine group, respectively. The carbonyl group of the acyl-hydrazone ligands does not participate in coordination in any of complexes **HL^{11}**–**HL^{14}**. The coordination mode of the ligands in all complexes could be established by comparing the IR and ^{1}H NMR spectra.

Formation of the hydrazonate complexes only proved possible with the derivatives of **HL^{22}**. A study of the corresponding single crystal showed the presence of the dimer $[Re_2(L^{22})_2(CO)_6]$, in which the phenolate group of the ligand of the dimer partner coordinates to rhenium after deprotonation. This same group is used to bind to the rhenium atom of the dimer partner at the position released by the halide.

1. Introduction

The coordination chemistry of rhenium continues to be of current interest because it is the main surrogate in the design of ^{99m}Tc complexes as possible drugs to perform radioimaging using the SPECT technique. Furthermore, since optimization of the production of the $\{Tc(CO)_3\}^+$ fragment in biologically compatible media [1], this latter coordinating center, and consequently its surrogate $\{Re(CO)_3\}^+$, has attracted great attention due to the important advantages when designing a radiopharmaceutical. In addition to their configurational robustness, the hydrophobic character of carbonyl groups, which facilitates their biodistribution, has been cited.

To help in the design of such complexes, intensive work has been carried out to determine which groups particularly favor their stabilization, and the particular stability of $\{M(CO)_3\}^+$ (M = Tc, Re) complexes with aromatic imines such as pyridine or imidazole [2] has been identified.

Another interesting property of the $\{Re(CO)_3\}^+$ fragment is its inertia, which allows the isolation of coordinated species that are difficult to observe with other metal centers [3].

Hydrazones are organic compounds containing the $R_2C = N\text{-}NH_2$ moiety [4]. Given their versatile properties and simple design and synthesis, their applications are of interest in different fields, such as analytical, organic, or medicinal chemistry. In the analytical chemistry field, these ligands present chelatometric properties, as reported by Katiyar and Tandon [5]. Spectrophotometric determination is the most common application of these systems, and they have been shown to be able to detect several different metals, including mercury [6], depending on the nature of the hydrazone.

The application of hydrazones in the pharmaceutical field stands out since these ligands exhibit a wide variety of biological activities (treatment of tuberculosis [7,8], intestinal antiseptics [9], antifungal agents [10], or antidepressants [11], amongst others), and these activities are often related to their coordination to a metallic center [8].

There are numerous literature references regarding active rhenium complexes with hydrazone ligands [12], and interesting biological

* Corresponding author at: Universidade de Vigo, Departamento de Química Inorgánica, Facultade de Química, 36310 Vigo, Spain.
E-mail address: ezequiel@uvigo.es (E.M. Vázquez-López).

https://doi.org/10.1016/j.poly.2022.115917
Received 8 March 2022; Accepted 13 May 2022
Available online 18 May 2022

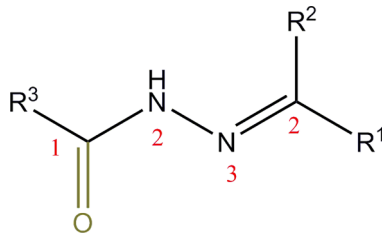

Scheme 1. The (acyl)-hydrazone ligand and atomic numbering scheme used in this work.

properties have been reported in some cases [13]. In this regard, acyl-hydrazones are an interesting type of hydrazone because the presence of the C1 = O group (Scheme 1) increases the acidity of the ligand (N2-H group) and its ability to form acyl-hydrazonate complexes, in addition to binding to the metal cation via the N3,O coordination mode [14]. In the past we have shown that, when one [3,15] or two [16] pyridine substituents are included on the *C*2 carbon (Scheme 1), the carbonyl oxygen atom is not involved in binding to the metal and the observed coordination mode is N3,N_{py} or N_{py},N_{py}'.

In the present work, we have designed and synthesized six new ligands bearing pyridine groups and/or acyl groups in different positions of the hydrazone chain (Scheme 2) to determine how these groups can affect the coordination mode of the ligand to rhenium(I) and, by extension, to the more relevant technetium(I) center from a bioinorganic point of view (Scheme 3).

2. Results and discussion

2.1. Synthesis and spectroscopic characterization

When designing ligands **HL^{11}**–**HL^{14}** (Scheme 2), we decided to include a 5-hydroxypyridine ring so that it may play a role in coordination to the metal together with the hydrazone chain. The substituents on *C*2 were chosen because they are susceptible to derivatization and/or able to interact with biomolecules [17]. **HL^{14}** is an exception as it contains another pyridine group. The four ligands were synthesized by reaction of 4-hydroxybenzaldehyde (**HL^{11}**), 2-fluoro-4-hydroxybenzaldehyde (**HL^{12}**), 2,4-dihydroxybenzaldehyde (**HL^{13}**) or 2-pyridinecarboxaldehyde (**HL^{14}**) with the previously synthesized 5-hydroxypicolinohydrazide. Details of the synthesis can be found in the experimental section. In the design of ligands **HL^{21}** and **HL^{22}**, we eliminated the carbonyl group of the hydrazone chain. These ligands can be easily obtained by treating the commercial reagent 2-hydrazino pyridine with the corresponding aldehyde (Scheme 2). A substituent derived from salicylaldehyde was included at C6 in **HL^{22}** to provide a possible coordination position after deprotonation.

All ligands were obtained in high yield as air-stable solids that are soluble in common polar organic solvents. Formation of the ligands was

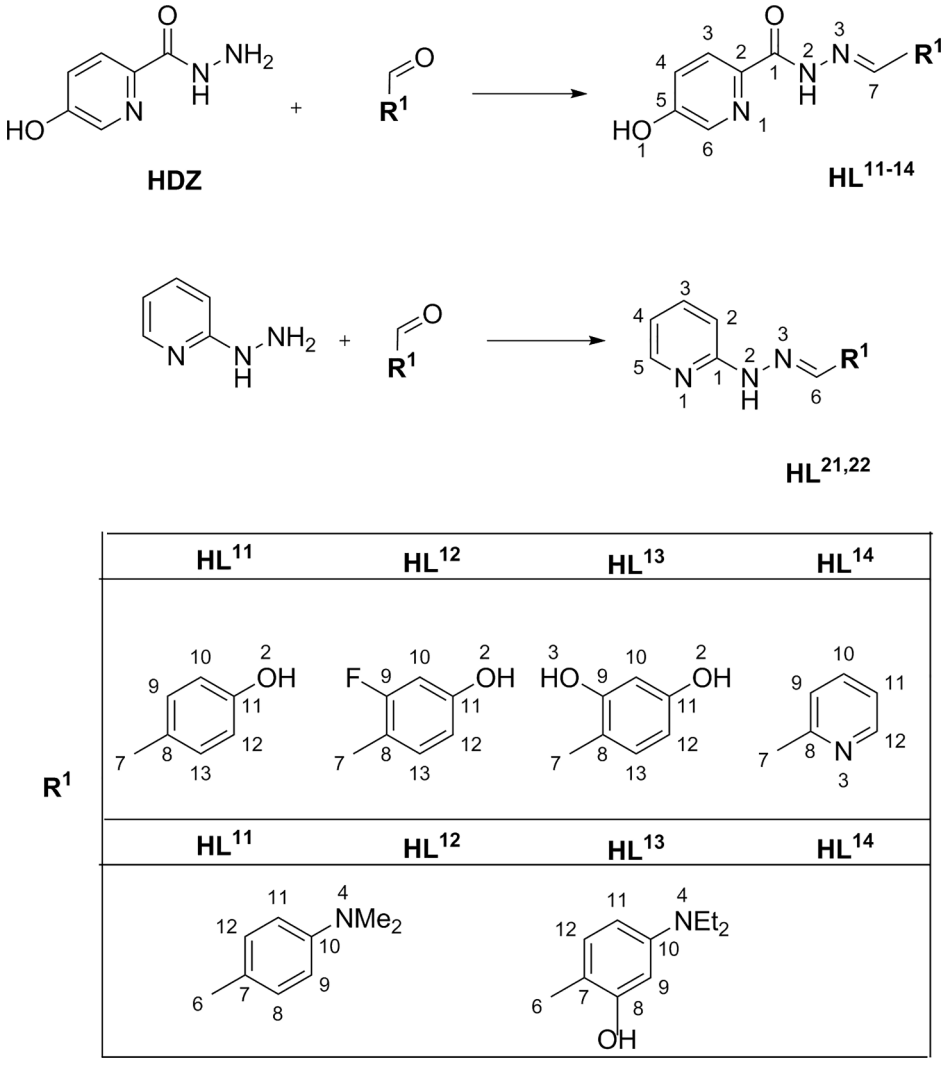

Scheme 2. Synthesis of ligands **HL^{11}**–**HL^{14}**, **HL^{21}**, and **HL^{22}** including the atomic numbering scheme used.

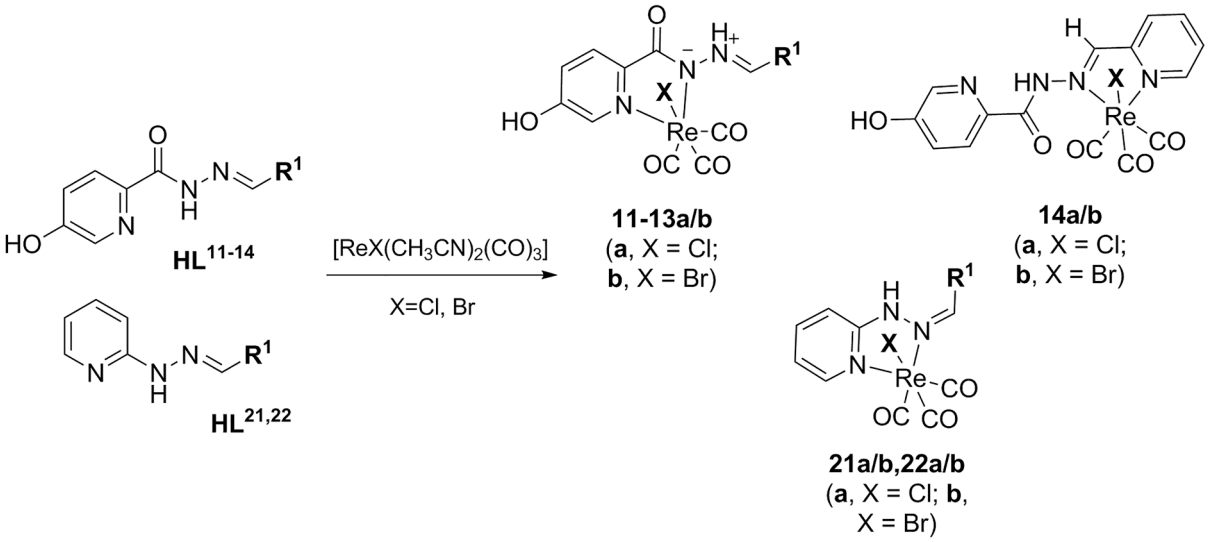

Scheme 3. Synthesis of the complexes.

confirmed by observation of the set of bands corresponding to the stretching modes for the acyl-hydrazone groups ν(C═O) and ν(C═N) at around 1650 and 1550 cm^{-1}, respectively. The ^{1}H NMR spectra of DMSO solutions are also characteristic, with the most downfield signals in the range 11.6–12.6 ppm due to the hydrazinic proton (N2-H in Scheme 1).

Twelve rhenium(I) complexes of stoichiometry [ReX(HL)(CO)$_3$] were obtained after refluxing *fac*-[ReX(CH$_3$CN)$_2$(CO)$_3$] (X = Cl, Br) with the corresponding ligand in ethanol (**HL^{11}**–**HL^{14}**) or chloroform (**HL^{21}**–**HL^{22}**) for 3–5 h. The proposed stoichiometry was confirmed by elemental analysis. Although most of the mass spectra showed peaks due to the species $|M-X|^{+}$ (sometimes as the base-peak), this behavior has been observed previously in rhenium(I) complexes containing Schiff bases such as acyl-hydrazones or thiosemicarbazones [15].

The *fac* configuration of the carbonyl groups in the $\{Re(CO)_3\}^{+}$ moiety was confirmed by observation of three strong/very strong bands in the 1820–2035 cm^{-1} range of the IR spectra (occasionally, the two lowest energy bands collapsed).

The study of the vibrational spectra of complexes containing ligands **HL^{11}**–**HL^{14}** focused on analysis of the medium frequency region (1700–1450 cm^{-1}), where we expect to see the bands attributable to the acyl-hydrazone group that will presumably show important differences

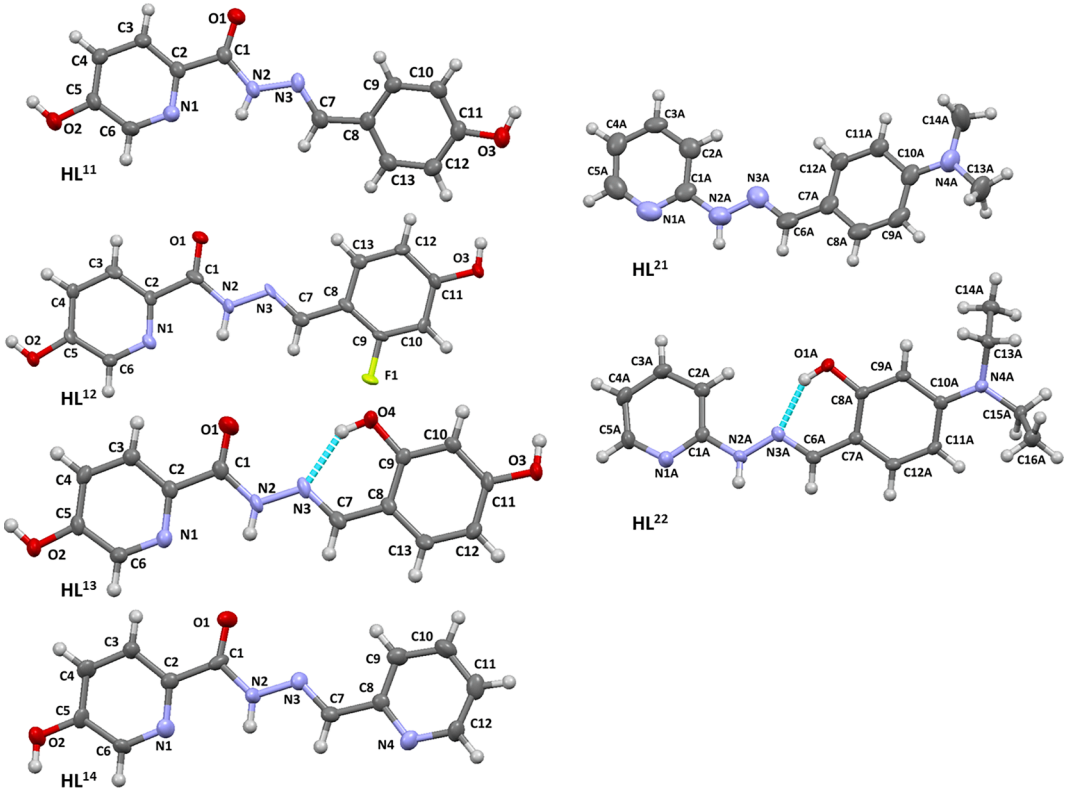

Fig. 1. Molecular structures of ligands **HL^{11}**–**HL^{22}**. Solvent molecules have been omitted for clarity. For the same reason, only one molecule of the asymmetric unit is depicted in **HL^{21}** and **HL^{22}**.

Table 1
Bond lengths (Å) and angles (°) for the ligands.

	HL^{11}	$HL^{12}·H_2O$	HL^{13}	HL^{14}	HL^{21} (a)	HL^{22}
O(1)-C(1)	1.2359(19)	1.228(5)	1.2331(19)	1.231(5)		
N(3)-C(7)	1.295(2)	1.282(6)	1.284(2)	1.291(5)		
N(3)-C(6)					1.247(2)	1.290(1)
N(3)-N(2)	1.3754(17)	1.375(5)	1.3760(16)	1.370(5)	1.372(2)	1.3780(9)
C(1)-N(2)	1.354(2)	1.355(6)	1.346(2)	1.363(5)	1.374(2)	1.367(1)
C(7)-N(3)-N(2)	113.00(13)	117.1(4)	117.62(13)	115.9(4)		
C(6)-N(3)-N(2)					116.6(1)	115.45(7)
O(1)-C(1)-N(2)	122.62(14)	123.4(4)	122.40(14)	122.6(4)		
O(1)-C(1)-C(2)	124.76(14)	122.7(4)	121.82(14)	122.3(4)		
N(2)-C(1)-C(2)	112.61(13)	114.0(4)	115.78(13)	115.1(4)	120.4(1)	122.64(7)
N(1)-C(1)-N(2)					117.4(1)	114.62(7)
N(3)-C(7)-C(8)	123.57(14)	120.2(4)	120.52(14)	120.1(4)		
N(3)-C(6)-C(7)					122.4(1)	122.77(8)
C(1)-N(2)-N(3)	121.70(13)	119.1(4)	118.78(13)	118.6(4)	120.1(1)	119.93(7)

(a). Mean value for the two molecules in the asymmetric unit obtained using the expression: $x = \Sigma x_j/(\sigma_j)^2$; $\sigma(x) = \Sigma 1/(\sigma_j)^2$.

due to the different coordination modes. Thus, the band at 1630–1660 cm^{-1} corresponding to the free ligand is displaced slightly to lower energies in complexes **11a,b**–**13a,b**, whereas in complexes **14a,b** this displacement is more pronounced (around 1700 cm^{-1}, see references [14] and [15]). This suggests that the coordination mode of the acyl-hydrazone is different in the latter compounds, as subsequently confirmed by X-ray single-crystal diffraction (vide infra). The other bands located in the range 1450–1620 cm^{-1} in the free ligands, and which have a high participation of vibrational modes related to the C═N bonds, are slightly displaced in complexes **11a**,**b**–**14a**,**b**. Similarly, in complexes **21** and **22** slight changes in the positions of the bands in the 1510–1635 cm^{-1} region with respect to free $\mathbf{HL^{21}}$ and $\mathbf{HL^{22}}$ can also be attributed to coordination.

We have previously reported the utility of using NMR spectroscopy to diagnose the acyl-hydrazone coordination mode in rhenium(I) complexes [16]. Indeed, our experience shows that the position of the N2-H proton is strongly dependent on the formation of the chelate with the acyl-hydrazone group. Similarly to what was observed for thiosemicarbazones, despite the slight deshielding of all signals for the ligand upon coordination (0.2–0.3 ppm), the N2-H proton signal is strongly shifted to low field (about 2 ppm) when the N3,O five-membered chelate ring is formed. In the case of complexes **14a**,**b** the hydrazinic N2-H is hardly shifted with respect to the free ligand, therefore this group does not form part of the chelate ring. In contrast, the most deshielded signals in $\mathbf{HL^{11}}$, $\mathbf{HL^{12}}$ and $\mathbf{HL^{13}}$ (at 11.66, 11.92 and 12.07 ppm, respectively) appear at around 11.46 and 11.60 ppm in complexes **11a,b**–**13a,b**, whereas the remaining signals are, as usual, slightly deshielded in the NMR spectra. These findings, together with those relating to the ν(C═O) band in the IR spectra, suggest that ligands $\mathbf{HL^{11}}$–$\mathbf{HL^{14}}$ are not linked to the rhenium in the usual O,N3-bidentate mode and that, in fact, the first three ligands coordinate differently to $\mathbf{HL^{14}}$. This can be explained by the presence of one ($\mathbf{HL^{11}}$–$\mathbf{HL^{13}}$) or two ($\mathbf{HL^{14}}$) pyridine groups, which implies greater coordination possibilities than those offered by the acyl-hydrazone group alone. It should also be noted that a characteristic of the ligand signals for $\mathbf{HL^{14}}$ when complexed is the deshielding of the signal due to the C7-H methylene group by more than 1 ppm (Scheme 2). This behavior is in accordance with coordination of the ligand via the azomethine nitrogen (N3) and the pyridine nitrogen (N4), thus menaing that the C7-H group forms part of the chelate ring. This latter mode was confirmed by single-crystal X-ray diffraction (vide infra).

As regards the complexes containing $\mathbf{HL^{21}}$ and $\mathbf{HL^{22}}$, deshielding of the signal due to the N2-H group (again by about 2 ppm) suggests coordination of the rhenium by N1 (pyridinic group) and N3 (azomethinic), thus forming a five-membered chelate ring.

Synthesis of the complexes in the presence of bases such as NEt_3 or NaOH to facilitate deprotonation of the ligands was tested. In general, it was difficult to isolate a pure solid and, with the exception of the derivative of $\mathbf{HL^{22}}$, the reaction mixtures do not appear to contain an identifiable stoichiometric product. The mass spectrum of product **22c** suggested the presence of $[Re_2(L^{22})_2(CO)_6]$ dimers, and an X-ray study of single crystals confirmed this hypothesis.

2.2. Crystal structures

The molecular structures of all ligands (Fig. 1) were determined by X-ray diffraction using single crystals obtained by slow evaporation of ethanol or acetone solutions. In some cases, the presence of twin crystals ($\mathbf{HL^{12}}$ and its complex **12a**) somewhat hindered an optimal refinement but, in general, the models obtained showed reasonable residual factors and gave meaningful structural data (Table 1).

Some of the aspects common to all the structures derived from 5-hydroxy-picolinohydrazide that we can highlight are: i) the rings connected by the acyl-hydrazone group are practically coplanar (with the greatest distortions being observed for $\mathbf{HL^{12}}$ but not exceeding 18°), and ii) the bond conformations follow the same pattern observed in other hydrazone ligands: C2-C1 (*E*), C1-N2 (*Z*), N2-N3 (*E*), N3-C7 (*E*) [for simplicity, the same notation (*Z* and *E*) will be used to identify both the type of isomer/configuration (for example, on the C7–N3 link) and the rotamer/conformer (as derived from the substituents on the N2–C1 link) along the acyl-hydrazone arm C7–N3–N2–C1(O1)–C2].

The C1–O1, C—N and N—N bond distances mainly suggest a double-bond character for the C7–N3 and C1–O1 linkages, although some π delocalization along the hydrazone chain is also possible [14].

The single crystals of the two ligands derived from 2-hydrazinopyridine ($\mathbf{HL^{21}}$ and $\mathbf{HL^{22}}$) contain two molecules per asymmetric unit (Fig. 2), differing only slightly in terms of the angles between the planes or the relative position of the terminal NR_2 groups, so we can consider them to be structurally equivalent. Both crystals belong to centrosymmetric groups ($P2_1/c$ for $\mathbf{HL^{21}}$ and *P*-1 for $\mathbf{HL^{22}}$), although we have not detected missed symmetry. Again, the values for the C—N and C—C distances along the hydrazone chain suggest some delocalization of π-electron density (even at the N—N link). This delocalization is probably also responsible for the co-planarity of the pyridine rings and the substituent at C6, although it should be mentioned that intramolecular hydrogen bonding involving the phenol group and the azomethinic nitrogen (O1A–H1A–N3A = 0.85, 1.90, 2.6658(13) Å, 149.0° and O1B–H1B–N3B = 0.85, 1.96, 2.7172(13) Å, 148.7°) in the $\mathbf{HL^{22}}$ ligand plays a role in the co-planarity of the entire molecule. The conformation in the C1–N2–N3–C6 hydrazone arm is *EEE* in both ligands.

In ligands $\mathbf{HL^{11\text{-}14}}$, molecules of both kinds of ligands are associated in the crystal via medium hydrogen bond type O—H..O involving the phenol (OH) and hydrazinic nitrogen (N2-H) as donor groups and the

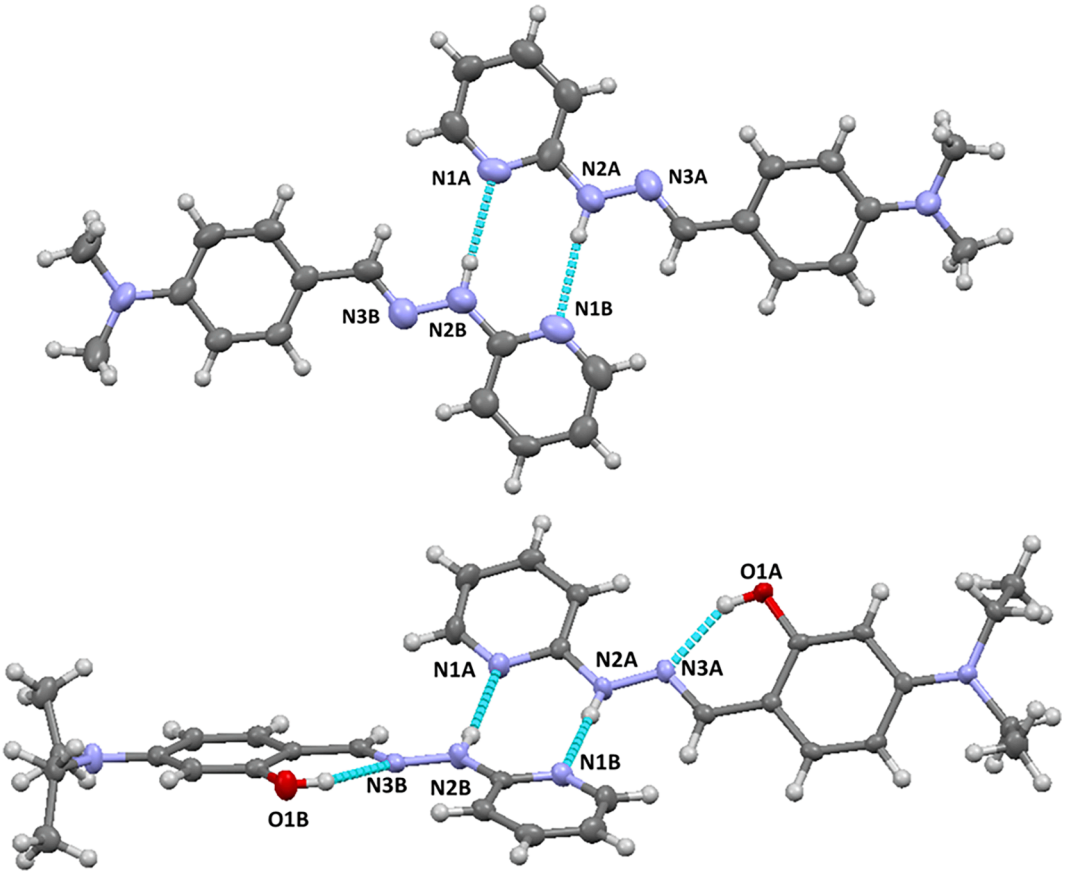

Fig. 2. Formation of dimers by H-bonding in $\mathbf{HL}^{21}$ (top) and $\mathbf{HL}^{22}$ (bottom).

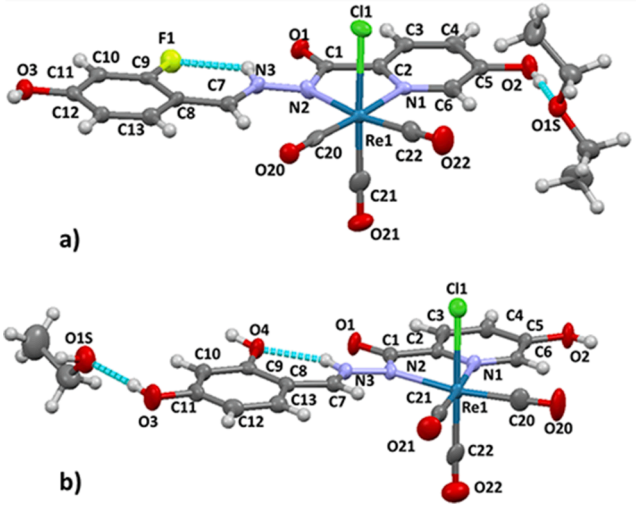

Fig. 3. The asymmetric unit in **12a**·(Et_2O) (a) and **13a**·(EtOH) (b).

carbonyl (C═O) and azomethinic nitrogen (N3) as acceptor groups. Depending on the number and relative distribution of those groups in each case, the dimensionality and topology of the chains is different (see Supplementary Material).

In ligands $\mathbf{HL}^{21\text{-}22}$, the two molecules in the asymmetric unit are associated via hydrogen bonds involving the hydrazine N2-H group of one and the pyridine nitrogen of the other (Fig. 2). This means that all the active groups are blocked by hydrogen bonding and, therefore, that the dimers formed are packed in the crystal via much weaker interactions.

Figs. 3 and 4 show the molecular structures of different [ReX(HL)$(CO)_3$] complexes, as determined by X-ray diffraction (Table 2). This technique allowed us to clarify the different spectroscopic behaviours of ligands $\mathbf{HL}^{11\text{-}13}$ in complexes with respect to those of $\mathbf{HL}^{14}$ and $\mathbf{HL}^{21\text{-}22}$.

Firstly, we can identify some elements that are common to all structures of the complexes included in this paper: i) the pyridine group is always involved in the coordination, as expected given the known affinity of the $\{M(CO)_3\}^+$ group (M = Tc, Re) for aromatic imines; ii) the ligand achieves the bidentate coordination mode by complementing the aforementioned pyridine with a hydrazone nitrogen. It is important to note that in the ligands derived from acyl-hydrazone ($\mathbf{HL}^{11}$–$\mathbf{HL}^{14}$), the carbonyl group never participates in rhenium coordination. This behaviour has been observed before in other acyl-hydrazonate complexes [2]; iii) the resulting chelate is always a five-membered ring even though other sizes, for example six-membered due to coordination via N_{py},N3, could be formed; iv) the coordination geometry around the rhenium cation can be described as octahedral, involving three carbon atoms in a *fac* configuration, two nitrogen atoms from the hydrazone ligand and the halogen atom. The main distortion of the ideal geometry is imposed by the chelate angle, which has a value of around 75°.

In most acyl-hydrazone complexes, coordination (with or without deprotonation) involves rotation of the C1–N2 bond so that the ligand binds to the metal via the O and N3 atoms. The coordinated ligands in **12a** and **13a** maintain the *EZEE* conformations observed in the crystal structure of the free ligands. This implies coordination to rhenium via the N1 pyridinic and N2 hydrazinic atoms and, consequently, rearrangement of the proton, which migrates to N3. This finding was confirmed by the successful isotropic refinement of H—N(3) in the model and agrees with the different chemical shift of the ^{1}H NMR signal. In addition, this finding confirms that ligands $\mathbf{HL}^{12}$ and $\mathbf{HL}^{13}$ (and $\mathbf{HL}^{11}$ based on the spectroscopic behavior of its complexes) behave as

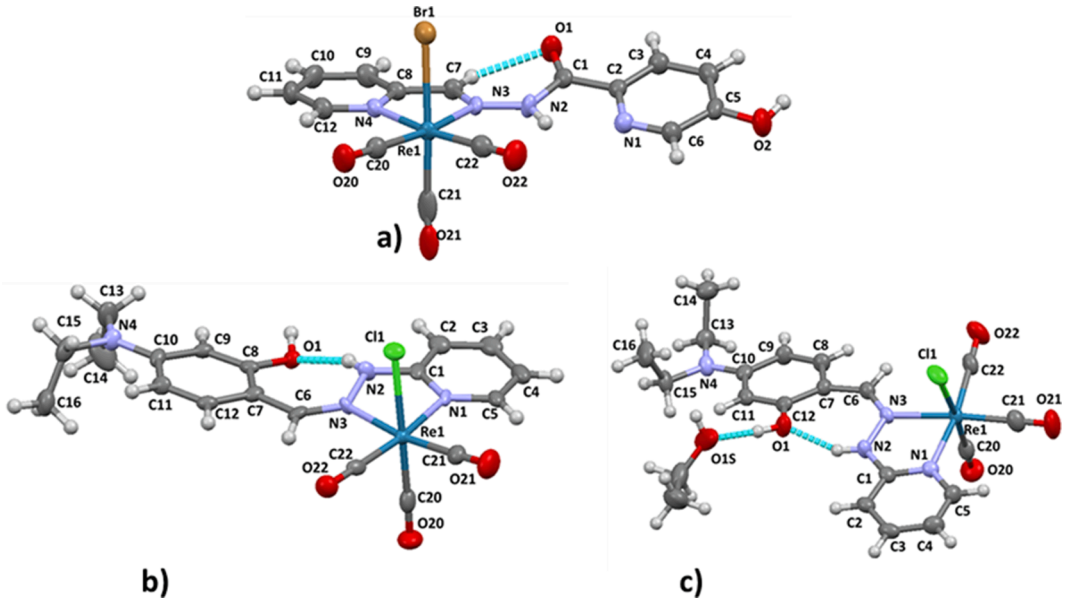

Fig. 4. The asymmetric unit in **14b** (a), **22a** (b) and **22a**·EtOH (c).

zwitterions. In both structures (**12a** and **13a**), the six-membered ring is formed via an intramolecular hydrogen bond involving the protonated group N3^{+}-H and the substituent in the *meta* position on the benzene linked to C7 (F in **12a** and O(H) in **13a**). This interaction likely plays an important role in stabilization of the zwitterion.

HL[14] offers a new coordination position for the rhenium cation due to the additional pyridine ring on the C7 carbon. As such, in complex **14b** we observe that the ligand is again bidentate (forming a five-membered ring) but coordinates via the pyridine nitrogen N4 and the azomethinic nitrogen N3 (Fig. 4a). To accomplish this, the N2–N3 bond must formally rotate (as must the C7–C8 bond), such that the C7-H group is now oriented toward the C═O carbonyl of the hydrazone chain. This allows the hydrogen-bonding interaction C7-H···O1 (0.90, 2.20, 2.802(5) Å, 120.5°). In any case, the C7-H group is integrated into the chelate ring and causes the greatest deshielding of the ^{1}H NMR signal with respect to other ligand protons in the spectra of **14b** and **14a**. The value of the Re–N3 distance—and this can be also observed in the structures of **22a** and **22b**—is equivalent to the Re–N2 distance observed in **12a** and **13a**, despite the anionic character of the donor nitrogen in the latter two complexes. The limited variation in hydrazone chain distances in rhenium complexes after deprotonation has also been reported previously [2].

Although the N–Re–N angle is statistically equivalent in all three acyl-hydrazone complexes, the two Re–N bond lengths in **14b** define a more symmetric "bite" because they are virtually identical. In contrast, when the bonding distances in the hydrazone chain of complexes **12a**, **13a** and **14b** are analyzed, it can be concluded that there are few statistically significant differences with respect to their free ligands, except for the elongation of the N2–N3 bond in the complexes.

Ligand **HL**[22] coordinate in a similar manner in the complex **22a** and its solvate **22a**·EtOH (Fig. 4b, c). Similar molecular connectivity was observed in the model obtained from single crystals of **21b** (Figure S1). However, the lack of quality of the diffractions data discouraged inclusion of the structure in the present article. Thus, these ligands bind to rhenium via the pyridine nitrogen (N1) and the azomethine nitrogen (N3) of the hydrazone chain, thus meaning that the N2-H groups form part of the chelate ring. The difference in the chemical shift of this proton in complexes **21a**,**b** and **22a**,**b** is likely due to the fact that the N2-H group is involved in an intramolecular hydrogen bond with the O1 (H) group in complexes **22**, as shown by the X-ray diffraction studies for **22a** (see Fig. 4c, d).

The coordination polyhedron in complexes **21b** and **22a** is very similar, with no relevant differences between the Re–N distances. As we observed for complexes of the acyl-hydrazone ligands, metalation does not seem to produce important modifications in the bond distances and angles in the hydrazone chain, except for the elongation of the N2–N3 distance.

The structure of dimer **22c** is shown in Fig. 5. The compound is formed by deprotonation of ligand **HL**[22] at the O1 group, with the hydrazone group (N2-H) remaining protonated. The O1 atom binds to the rhenium cation of the dimer partner at the position vacated by the halide. In this way, the hydrazonate ligand maintains its planarity while coordination via the pyridine N1 and azomethine N3 atoms is also maintained. In fact, the Re–N distances, as well as those involved in the C6-N3-N2-C1 chain, are similar to those in **22a**, thus indicating that the hydrazone group is barely affected by deprotonation.

As a consequence of the deprotonation of the O1-H, the intramolecular hydrogen bond established (as acceptor, Fig. 4c) with N2-H in **22a** (N2-H2···O1 = 0.849(19), 1.87(3), 2.668(5) Å, 156(5)°, similar to the values for **22a**·**EtOH**), is clearly reinforced in **22c**, as can be observed by the decrease in the distance N2···O1 (N2-H2···O1 = 0.84, 1.72, 2.522(3) Å, 159.7°).

3. Conclusion

We have described a study of the coordinative preferences of the {Re(CO)$_3$}$^{+}$ fragment with respect to six different hydrazone ligands containing pyridine and acyl groups in coordinative positions. We have found that the rhenium cation always binds to the nitrogen atom of one of the pyridine groups and "ignores" the oxygen atom of the hydrazone group (if present) by forming a chelate ring with one of the nitrogen atoms of the hydrazine fragment. The chelate ring is always five-membered even when, as can be seen in structures **12a** and **13a**, this forces the reorganization of the hydrazinic hydrogen, thus leading to the formation of a zwitterion form [-N^{-}—N^{+}(H) =] in the coordinated hydrazone.

Although these conclusions can be drawn from the X-ray diffraction study of the majority of the twelve complexes synthesized, the spectroscopic results, fundamentally ^{1}H NMR, allow them to be extrapolated to those compounds that we have not been able to crystallize.

Table 2
Bond lengths (Å) and angles (°) for the complexes.

	12a.Et_2O	13a·EtOH	14b	22a	22a.EtOH	22c.2$CHCl_3$
X =	Cl	Cl	Br	Cl	Cl	O(1)$^{\#1\ (a)}$
Re(1)-N(2)	2.168(7)	2.1838(19)				
Re(1)-N(1)	2.195(6)	2.1948(18)		2.169(4)	2.160(3)	2.1589(19)
Re(1)-N(4)			2.170(4)			
Re(1)-N(3)			2.176(4)	2.173(4)	2.180(3)	2.176(2)
Re(1)-X(1)	2.495(2)	2.4842(6)	2.6170(5)	2.5069(12)	2.5029(9)	2.1581(16)
O(1)-C(1)	1.224(10)	1.248(3)	1.216(5)			
N(3)-C(7)	1.297(10)	1.290(3)	1.292(6)			
N(3)-C(6)				1.300(6)	1.298(4)	1.300(3)
N(3)-N(2)	1.381(10)	1.381(2)	1.373(5)	1.382(5)	1.410(4)	1.394(3)
N(2)-C(1)	1.366(10)	1.351(3)	1.382(5)	1.365(6)	1.342(4)	1.359(3)
N(2)-Re(1)-N(1)	73.7(3)	74.06(7)				
N(4)-Re(1)-N(3)			74.07(13)			
N(1)-Re(1)-N(3)				74.98(14)	75.21(10)	75.26(7)
N(2)-Re(1)-X(1)	84.21(19)	83.63(5)				
N(3)-Re(1)-X(1)			85.33(9)	83.05(10)	85.90(7)	80.50(7)
N(1)-Re(1)-X(1)	82.59(18)	85.66(5)		85.84(10)	81.92(8)	79.66(7)
N(4)-Re(1)-X(1)			84.34(9)			
C(7)-N(3)-N(2)	125.3(7)	125.8(2)	120.6(4)			
C(1)-N(2)-N(3)	108.5(6)	110.27(18)	127.9(4)	118.2(4)	117.8(3)	117.19(19)
C(1)-N(2)-Re(1)	119.7(5)	118.50(14)				
N(2)-N(3)-Re(1)			121.4(3)	112.3(3)	112.68(19)	113.41(14)
N(3)-N(2)-Re(1)	131.2(5)	131.20(14)				
O(1)-C(1)-N(2)	124.9(7)	124.6(2)	124.4(4)			
O(1)-C(1)-C(2)	122.6(7)	121.4(2)	124.3(4)			
N(2)-C(1)-C(2)	112.5(7)	113.97(19)	111.4(4)			

a). Symmetry transformations #1−x + 1, −y + 1, −z + 1.

4. Experimental section

4.1. Materials and physical measurements

The starting materials and solvents were obtained commercially and were used as supplied. The adducts [ReX(CO)$_3$(CH$_3$CN)$_2$] (X = Cl, Br) were synthesized following the methods of Farona and Kraus [18] from the corresponding [ReX(CO)$_5$] (X = Cl, Br) compounds [19]. Elemental analyses (C, H, N, S) were carried out using a FlashEA 1112 Series microanalyser. IR spectra were recorded in the solid phase by ATR (4000–400 cm^{-1}) using a Jasco FT/IR-6100 spectrophotometer. ^{1}H NMR spectra were obtained using a Bruker AMX 400 spectrometer. Mass spectra (ESI +) were recorded using a microTOF-Focus (Bruker Daltonics) mass spectrometer.

4.2. Crystallography

The crystallographic data were collected at 100 K using a Bruker D8 Venture diffractometer with a Photon 100 CMOS detector and Mo-Kα radiation (λ = 0.71073 Å) generated by an Incoatec high brillance microfocus source equipped with Incoatec Helios multilayer optics. The APEX3 software was used to collect frames of data, index reflections, and determine the lattice parameters, SAINT was used for integration of the intensity of reflections, and SADABS for scaling and empirical absorption correction [20]. The structures were solved using the SHELXT program [21]. All non-hydrogen atoms were refined on F^2 with anisotropic thermal parameters using SHELXL [22]. Hydrogen atoms were inserted at calculated positions and refined as riding atoms except those bonded to heteroatoms (N—H and O—H) which were generally located from the electron density synthesis Fo-Fc map and isotropically refined. Validation checking of the models (including for missed symmetry) was performed using PLATON [23] and plots of all structures were produced using MERCURY [24] with a 50% of thermal ellipsoid probability level. The crystallographic data collection and refinement parameters are listed in Table S1.

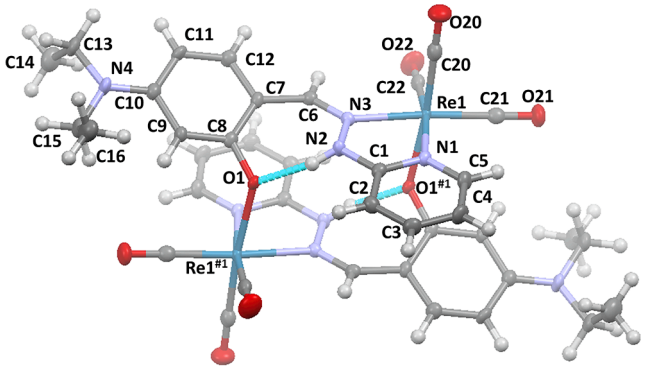

Fig. 5. The dimer molecular unit in **22c·2CHCl$_3$**, with the solvent molecule omitted for clarity.

All crystals of **HL**[12] and **12a** were non-merohedral twins and two components were identified using the CELL_NOW program [25]. After reduction, absorption corrections were performed with TWINABS [26]. Data containing the reflections of the main component were used to solve the structure but both domains were included in the final refinement.

4.3. Synthesis of 5-hydroxy-picolinohydrazide

This hydrazide was synthesised in two steps, namely esterification of the commercial carboxylic acid [27] then conversion of this methyl ester (**EST**) into the corresponding hydrazide.

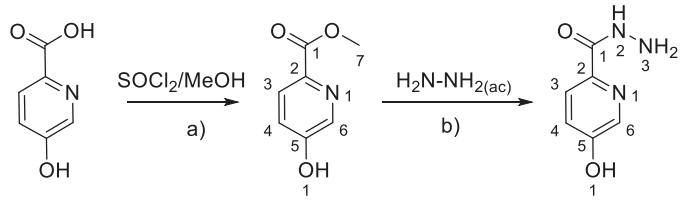

a) Thionyl chloride (8 mL, 107.6 mmol) was added dropwise to a suspension of 5-hydroxy-picolinoylic acid monohydrate (2 g, 12.7 mmol) in dry MeOH (40 mL) under an argon atmosphere and the mixture was refluxed for 17 h. NaOH was then added until pH 7. The white solid precipitated was filtered off and vacuum dried over $CaCl_2$/KOH.

b) A solution of aqueous hydrazine (0.5 mL, 8.0 mmol) was added to a suspension of methyl 5-hydroxy-picolinate (**EST**) (150 mg, 1.0 mmol) in $CHCl_3$ (5 mL) and the mixture stirred at room temp. for 24 h. The white solid formed was filtered off and vacuum dried over $CaCl_2$/KOH.

HDZ crystals were obtained by slow evaporation of a solution in methanol at 4 °C.

Details of the analytical and spectroscopic characterization of these compounds are included in the Supplementary Material.

4.4. Synthesis of the ligands

5-Hydroxy-picolinoyl hydrazide (HDZ) for $\mathbf{HL^{11\text{-}14}}$, or 2-hydrazinopyridine for $\mathbf{HL^{21,22}}$, and the corresponding benzaldehyde were refluxed for 4 h in an alcohol medium after addition of two drops of glacial acetic acid. The solids formed were filtered off and vacuum dried over $CaCl_2$/KOH.

Details of the analytical and spectroscopic characterization (MS, IR and NMR) of each of the ligands as well as the methods for obtaining single crystals are included in the Supplementary Material.

4.5. Synthesis of the hydrazone complexes

A solution of *fac*-[ReX$(CH_3CN)_2(CO)_3$] (X = Cl, Br) and the corresponding ligand $\mathbf{HL^n}$ in ethanol ($\mathbf{HL^{11\text{-}14}}$) or chloroform ($\mathbf{HL^{21\text{-}22}}$) was refluxed for 3–5 h. The resulting solution was concentrated in vacuum and stored at 4 °C after addition of diethyl ether. The solid formed was washed with water, filtered off and vacuum dried over $CaCl_2$/KOH.

Details of the analytical and spectroscopic characterization (MS, IR and NMR) of each of the complex as well as the methods for obtaining single crystals are included in the Supplementary Material.

4.6. Synthesis of the hydrazonate complex

A solution of $\mathbf{HL^{22}}$ (43 mg, 0.15 mmol) and *fac*-[ReCl$(CH_3CN)_2(CO)_3$] (59 mg, 0.15 mmol) in ethanol (15 mL) was refluxed for one hour. A solution of NaOH (31 mg, 0.78 mmol) in water (5 mL) was then added and the mixture refluxed for a further 2 h. The orange solid formed was filtered off and vacuum dried over $CaCl_2$/KOH.

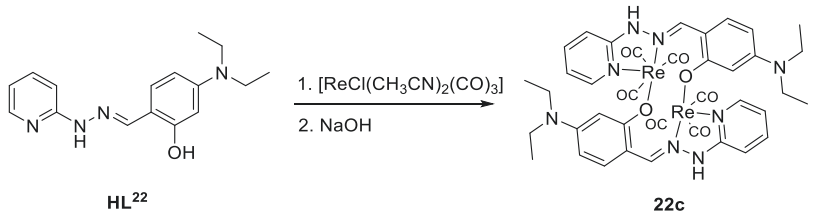

Details of the analytical and spectroscopic characterization (MS, IR and NMR) of this compound are included in the supplementary material.

CRediT authorship contribution statement

Saray Argibay: Formal analysis, Writing – original draft. **Diego Costas-Riveiro:** Formal analysis, Writing – original draft. **Rosa Carballo:** Formal analysis, Conceptualization, Supervision, Writing – review & editing. **Ezequiel M. Vázquez-Vázquez:** Conceptualization, Supervision, Formal analysis, Resources, Funding acquisition, Writing – original draft, Writing – review & editing.

Declaration of Competing Interest

The authors declare that they have no known competing financial interests or personal relationships that could have appeared to influence the work reported in this paper.

Acknowledgements

Financial support from the Ministerio de Ciencia e Innovación (Spain) under research project PID2019-110218RB-I00 is gratefully acknowledged. We thank the Structural Determination Service of the Universidade de Vigo-CACTI for X-ray diffraction measurements.

Funding for open access charge: Universidade de Vigo/CISUG.

Appendix A. Supplementary data

CCDC-2157038 to 2157047 and CCDC 215749 to 2157051 (see Table S1) contain the supplementary crystallographic data for this

paper. These data can be obtained free of charge via http://www.ccdc.cam.ac.uk/conts/retrieving.html, or from the Cambridge Crystallographic Data Centre, 12 Union Road, Cambridge CB2 1EZ, UK; fax: (+44) 1223-336-033; or e-mail: deposit@ccdc.cam.ac.uk. Supplementary data to this article can be found online at https://doi.org/10.1016/j.poly.2022.115917.

References

[1] R. Alberto, The particular role of radiopharmacy within bioorganometallic chemistry, J. Organomet. Chem. 692 (2007) 1179–1186, https://doi.org/10.1016/j.jorganchem.2006.11.019.

[2] (a) J. Grewe, A. Hagenbach, B. Stromburg, R. Alberto, E.M. Vázquez-López, U. Abram. **Tricarbonyl Complexes of Rhenium(I) with Acetylpyridine Benzoylhydrazone and Related Ligands**. Z. Anorg. Allg. Chem. 629 (2003) pp. 303-311, and references therein, DOI: 10.1002/zaac.200390048. (b) M. Emami, H. Shahroosvand, R. Bikas, T. Lis, C. Daneluik, M. Pilkington. **Synthesis, Study, and Application of Pd(II) Hydrazone Complexes as the Emissive Components of Single-Layer Light-Emitting Electrochemical Cells**. Inorg. Chem. 60 (2021) pp. 982-994, DOI: 10.1021/acs.inorgchem.0c03102.

[3] S. Argibay-Otero, A. Graña, R. Carballo, E.M. Vázquez-López, Synthesis of novel dinuclear N-substituted-(4-methylaminobenzaldehyde) thiosemicarbazonates rhenium(I): formation of four- and/or five-membered chelate rings, conformation analysis and reactivity, Inorg. Chem. 59 (2020) 14101–14117, https://doi.org/10.1021/acs.inorgchem.0c01887.

[4] T.N. Sorrell, Organic Chemistry 2Ed, University Science Books, California, 2006.

[5] T.S. Katiyar, S.N. Tandon, 1-Isonicotinoyl-2-salicylidenehydrazine as a new chelatometric reagent, Talanta 11 (1964) 892–894, https://doi.org/10.1016/0039-9140(64)80118-1.

[6] G.S. Vasilikiotis, Analytical applications of isonicotinoyl hydrazones: I. A new selective reagent for mercury, Microchem. J. 13 (1968) 526–528, https://doi.org/10.1016/0026-265X(68)90028-3.

[7] C.M. Clark, D.F. Elmendorf, W.U. Cawthon, C. Muschenheim, W. McDermott, Isoniazid (isonicotinic acid hydrazide) in the treatment of miliary and meningeal tuberculosis, Am. Rev. Tuberc. 66 (1952) 391–415.

[8] J. Patole, U. Sandbhor, S. Padhye, D.N. Deobagkar, C.E. Anson, A. Powell, Structural chemistry and In vitro antitubercular activity of acetylpyridine benzoyl hydrazone and its copper complex against Mycobacterium smegmatis, Bioorg. Med. Chem. Lett. 13 (2003) 51–55, https://doi.org/10.1016/s0960-894x(02)00855-7.

[9] B. Begovic, S. Ahmedtagic, L. Calkic, M. Vehabović, S.B. Kovacevic, T. Catic, M. Mehic, Open clinical trial on using nifuroxazide compared to probiotics in treating acute diarrhoeas in adults, Mater. Sociomed. 28 (2016) 454–458, https://doi.org/10.5455/msm.2016.28.454-458.

[10] D. Secci, B. Bizzarri, A. Bolasco, S. Carradori, M. D'Ascenzio, D. Rivanera, E. Mari, L. Polletta, A. Zicari, Synthesis, anti-Candida activity, and cytotoxicity of new (4-(4-iodophenyl)thiazol-2-yl)hydrazine derivatives, Eur. J. Med. Chem. 53 (2012) 246–253, https://doi.org/10.1016/j.ejmech.2012.04.006.

[11] O. Benkert, A. Szegedi, M.J. Müller, Antidepressant Drugs in "International Encyclopedia of the Social & Behavioral Sciences", in: International Encyclopedia of the Social & Behavioral Sciences, Elsevier, 2001, pp. 529–535.

[12] P. Barbazán, R. Carballo, B. Covelo, C. Lodeiro, J.C. Lima, E.M. Vázquez-López, Synthesis, characterization, and photophysical properties of 2-hydroxybenzaldehyde [(1E)-1-pyridin-2-ylethylidene]hydrazone and its rhenium(I) complexes, Eur. J. Inorg. Chem. 2008 (17) (2008) 2713–2720.

[13] I. Picón-Ferrer, F. Hueso-Ureña, N.A. Illán-Cabeza, S.B. Jiménez-Pulido, J. M. Martínez-Martos, M.J. Ramírez-Expósito, M.N. Moreno-Carretero, Chloro-fac-tricarbonylrhenium(I) complexes of asymmetric azines derived from 6-acetyl-1,3,7-trimethylpteridine-2,4(1H,3H)-dione with hydrazine and aromatic aldehydes: Preparation, structural characterization and biological activity against several human tumor cell lines, J. Inorg. Biochem. 103 (2009) 94–100, https://doi.org/10.1016/j.jinorgbio.2008.09.014.

[14] P. Barbazán, R. Carballo, U. Abram, G. Pereiras-Gabián, E.M. Vázquez-López, Synthesis and characterization of ferrocenylcarbaldehyde benzoylhydrazone and its rhenium(I) complex, Polyhedron 25 (2006) 3343–3348, https://doi.org/10.1016/j.poly.2006.06.007.

[15] P. Barbazán, R. Carballo, I. Prieto, M. Turnes, E.M. Vázquez-López, Synthesis and characterization of several rhenium(I) complexes of 2-acetylpyridine and ferrocenyl carbaldehyde derivatives of 2-hydroxybenzoic acid hydrazide, J. Organomet. Chem. 694 (19) (2009) 3102–3111.

[16] P. Barbazán, A. Hagenbach, E. Oehlke, U. Abram, R. Carballo, S. Rodríguez-Hermida, E.m., Vázquez López, Tricarbonyl Rhenium(I) and Technetium(I) Complexes with Hydrazones Derived from 4,5-Diazafluoren-9-one and 1,10-Phenanthroline-5,6-dione, Eur. J. Inorg. Chem. (2010) 4622–4630, https://doi.org/10.1002/ejic.201000522.

[17] A. Nuñez-Montenegro, R. Carballo, E.M. Vázquez-López, Synthesis, Characterization and Binding Affinities for Estrogen Receptor (α/β) of Rhenium(I) Thiosemicarbazone Complexes, J. Inorg. Biochem. 140 (2914) pp. 53-63- DOI: 10.1016/j.jinorgbio.2014.06.012.

[18] M.F. Farona, K.F. Kraus, Coordination of organonitriles through CN.pi. systems, Inorg. Chem. 9 (1970) 1700–1704, https://doi.org/10.1021/ic50089a018.

[19] P. Schmidt, W.C. Trogler, F. Basolo, **Inorganic Syntheses: Reagents for Transition Metal Complex and Organometallic Syntheses**. R.J. Angelici, (Ed) Inorg. Synth. 28 (1990) pp. 160 –165, DOI: 10.1002/9780470132593.

[20] (a) Bruker. APEX3, SAINT and SADABS. Bruker AXS Inc, Madison , Wisconsin, USA, 2015.(b) L. Krause, R. Herbst-Irmer, G.M. Sheldrick, D. Stalke, D. **Comparison of silver and molybdenum microfocus X-ray sources for single-crystal structure determination**. J. Appl. Crystallogr. 48 (2015) pp. 3-10, DOI: 10.1107/S1600576714022985.

[21] G.M. Sheldrick, Shelxt,, **– Integrated space-group and crystal-structure determination**, Acta Crystallogr A 71 (2015) 3–8, https://doi.org/10.1107/S2053273314026370.

[22] G.M. Sheldrick, A short history of SHELX, Acta Crystallogr. A 64 (2008) 112–122, https://doi.org/10.1107/S0108767307043930.

[23] A.L. Spek, Structure validation in chemical crystallography, Acta Crystallogr. D65 (2009) 148–155, https://doi.org/10.1107/S090744490804362X.

[24] C.F. Macrae, P.R. Edgington, P. McCabe, E. Pidcock, G.P. Shields, R. Taylor, M. Towler, J. van de Streek, Mercury: visualization and analysis of crystal structures, J. Appl. Cryst. 39 (2006) 453–457, https://doi.org/10.1107/S002188980600731X.

[25] G.M. Sheldrick, CELL_NOW, Georg-August-Universität, Göttingen, Germany, 2008.

[26] G.M. Sheldrick, TWINABS 2012/1, Bruker, Madison, Wisconsin, USA, 2012.

[27] D.A. Claremon, L.W. Dillard, C. Dong, Y. Fan, S.D. Lotesta, A, Marcus, S.B. Singh, M.C. Tice, J. Yuan, W. Zhao, Y. Zheng, L. Zhuang, **Thiazolopyrrolidine inhibitors of ROR-gamma**. Patent WO 2014/179564 A1, 2014.